# Kinetic profiles and impurity transport response to 3D-field triggered ELMs in NSTX

F. Scotti[1], V.A. Soukhanovskii[1], J.M. Canik[2], R.E. Bell[3], A. Diallo[3], S.P. Gerhardt[3], W. Guttenfelder[3], S.M. Kaye[3], B.P. LeBlanc[3], M. Podestà[3]
(email: fscotti@pppl.gov)
[1]Lawrence Livermore National Laboratory, Livermore CA 94550, USA
[2]Oak Ridge National Laboratory, Oak Ridge TN 37831, USA
[3]Princeton Plasma Physics Laboratory, Princeton NJ 08543, USA

The response of kinetic plasma profiles to 3D-field triggered edge localized modes (ELMs) and the inter-ELM impurity transport were analyzed in lithium-conditioned H-mode discharges in NSTX. The ability to control the size and frequency ($f_{ELM}$) of ELMs will be critical in future devices, such as ITER, in order to avoid impurity accumulation and damage to wall and divertor plasma facing components (PFCs) due to large ELMs. Edge impurity flushing increased with $f_{ELM}$, with a progressive reduction in the carbon density $n_C$ inside the pedestal top. The ELM effect on the $n_C$ profiles was reproduced in MIST simulations with an inward convective perturbation and an outward diffusive/convective perturbation (inside and outside normalized volumetric radii $R_{VOL}$ =0.6, respectively). The increase in $f_{ELM}$ progressively affected inter-ELM kinetic profiles, with electron pressure $p_e$ inside the pedestal top reduced up to 40% for $f_{ELM}$=60Hz. The agreement of inter-ELM carbon transport with neoclassical estimates improved with the increase in $f_{ELM}$, similarly to what observed in naturally ELMy discharges [1].

ELM-free lithium-conditioned H-mode discharges in NSTX were characterized by core accumulation of impurities as a result of near-neoclassical impurity transport, an edge inward impurity pinch and the absence of edge flushing mechanisms (e.g., ELMs) [1]. Accumulation of metallic impurities led to core radiated power reaching up to 50% of the injected power, while accumulation of carbon led to uncontrolled $n_e$. The combined use of lithium coatings for deuterium control and ELM-triggering (via 3D-fields or granule injection) to flush core impurities is one of the candidate density control strategies for the NSTX-Upgrade (NSTX-U). Non-axisymmetric magnetic perturbations (n=3) were applied in NSTX to trigger ELMs ($f_{ELM}$=10-62.5 Hz), and mitigate core impurity buildup maintaining the positive effects of lithium on energy confinement [2, 3, 4].

The increase in $f_{ELM}$ progressively increased impurity flushing and modified edge plasma profiles. For ELMs triggered at 10Hz, carbon flushing was observed following the ELM crash for $R_{VOL}$ larger than 0.6. Up to a 30% drop in $n_C$ was observed at the pedestal top, with comparable effects in the $n_e$, $T_i$, $v_\phi$ profiles. While $n_C$ profiles recovered within the 100 ms ELM cycle, the increase in $f_{ELM}$ led to a reduction in the overall core carbon inventory $N_C$ progressively affecting $n_C$ at inner radii (Figure 1). In particular, $N_C$ decreased by up to a factor of two for $R_{VOL}$>0.5 with the increase in $f_{ELM}$ while no decrease was observed inside $R_{VOL}$~0.5. While $T_e$ profiles were mostly unchanged by the $f_{ELM}$ increase, $n_e$ and $p_e$ were reduced up to 40% at $\Psi_N$=0.6 but unaffected in the steep gradient region (Figure 2).

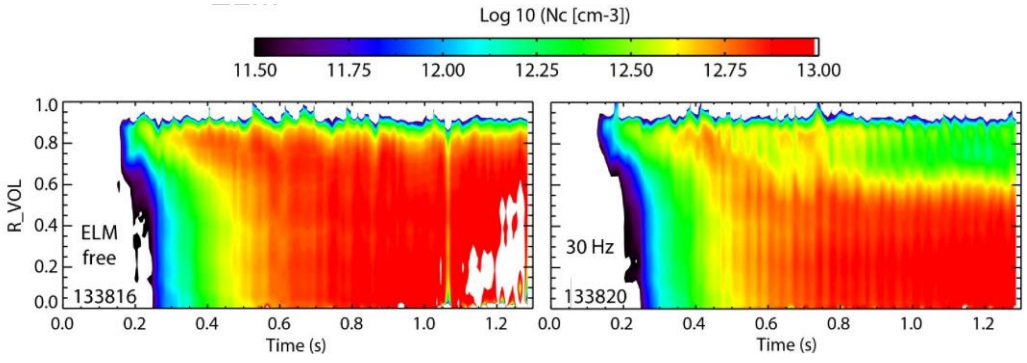


Figure 1: Carbon density for an ELM-free discharge (left) and a discharge with 30 Hz triggered ELMs (right)

Transient perturbations to the steady state particle diffusivity $D_C$ and convective velocity $v_C$ were applied in the impurity transport code MIST to simulate the response of the $n_C$ profile to ELMs. The equilibrium v/D ratio was inferred from the steady state $n_C$ profiles and the absolute values were scaled by the neoclassical diffusivity. The experimentally observed increase in core $n_C$ following the ELM was simulated with an inward convective perturbation for $R_{VOL}<0.6$. An outward (diffusive/convective) perturbation for $R_{VOL}>0.6$ was used in the simulation to reproduce the edge ELM flushing.

The agreement of inter-ELM carbon transport with neoclassical estimates improved with the increase in $f_{ELM}$. In NSTX H-mode discharges, intrinsic carbon transport was consistent with neoclassical estimates in ELMy discharges with boronized PFCs. Changes in $T_i$, $n_D$ profiles due to the application of lithium led to changes in carbon neoclassical convection. However, a deviation of carbon transport from neoclassical estimates was evident at the top of the pedestal, where a predicted inward pinch was not observed experimentally [1]. The application of 3D-field triggered ELMs to naturally ELM-free discharges led to changes in $n_e$, $T_i$, $v_\phi$ with the $v_\phi$ and $T_i$ normalized gradients increased by up to a factor of 3 at $R_{VOL}$ ~0.6 and 0.7, respectively. The changes in $T_i$ and $n_D$ profiles due to triggered ELMs led to changes in carbon neoclassical transport coefficients comparable and opposite to those observed with the transition from ELMy boronized discharges to ELM-free lithium-conditioned discharges (Figure 3), resulting in a sign change in $v_C$ at the top of the pedestal (from inward to outward convection). Concomitantly, better agreement between the neoclassical transport predictions (via the NCLASS code) and experimental $n_C$ profile shapes was observed in lithium-conditioned discharges with triggered ELMs in a similar way to naturally ELMy discharges, as shown in Figure 4 from the comparison between experimental peaking factors ($\nabla n_C / n_C$) and the neoclassical v/D.

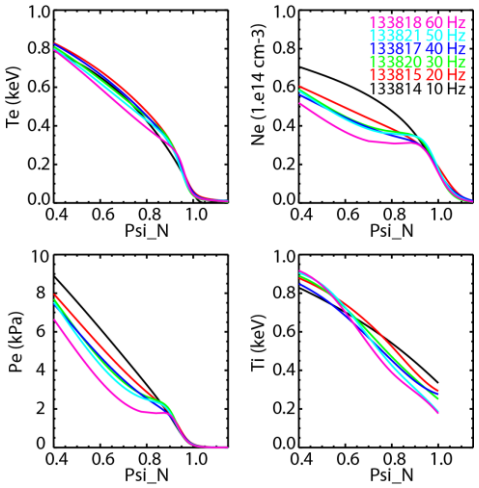


Figure 2: Evolution of inter-ELM kinetic profiles for $f_{ELM}$ = 10-60 Hz

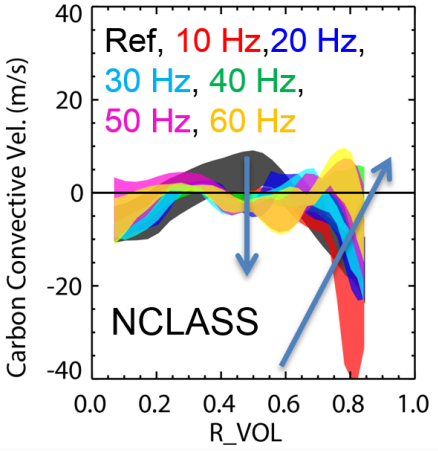


Figure 3: Carbon convective velocity as estimated from NCLASS for $f_{ELM}$ = 0-60 Hz

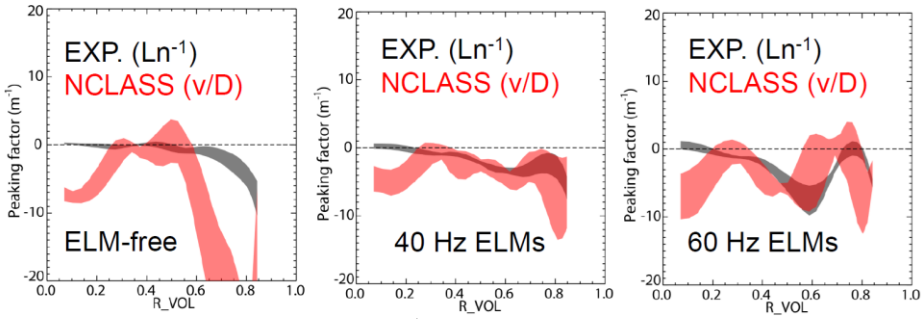


Figure 4: Experimental peaking factors ($Ln_C^{-1}$) in black and neoclassical predictions for the v/D ratio based on NCLASS calculations in red: ELM-free (left), 40 Hz (center), 60 Hz triggered ELMs (right).

Work supported by US DOE contracts DE-AC02-09CH11466, DE-AC05-00OR22725, DE-AC52-07NA27344.

[1] F. Scotti, et al., Nucl. Fusion 53 083001 (2013).
[2] J.M. Canik, et al, Phys. Rev. Letter 104 (4), 045001(2010).
[3] J.M. Canik et al., Nucl. Fusion 50 (3), 034012 (2010).
[4] J.M. Canik, et al., Nucl. Fusion 50 (6), 064016 (2010).